RVC OPEN ACCESS REPOSITORY

This author's accepted manuscript may be used for non-commercial purposes in accordance with Wiley Terms and Conditions for Self-Archiving.

The full details of the published version of the article are as follows:

TITLE: Species-specific consequences of an E40K missense mutation in superoxide dismutase 1 (SOD1)

AUTHORS: Draper, A C E; Wilson, Z; Maile, C A; Faccenda, D; Campanella, M; Piercy, R J

JOURNAL: FASEB Journal

PUBLISHER: Wiley

PUBLICATION DATE: 25 November 2019

DOI: https://doi.org/10.1096/fj.201901455R

RVC Royal Veterinary College University of London

Species-specific consequences of an E40K missense mutation in superoxide dismutase 1 (SOD1)

Alexandra CE Draper[1], Zoe Wilson[1], Charlotte Maile[1], Danilo Faccenda[2], Michelangelo Campanella[2, 3] & Richard J Piercy[1]

1: Comparative Neuromuscular Disease Laboratory, Royal Veterinary College, University of London, UK

2: Mitochondrial Cell Biology and Pharmaceutical Research Unit, Department of Comparative Biomedical Sciences, Royal Veterinary College, University of London, UK

3: UCL Consortium for Mitochondrial Research, Gower Street, NW1 0TU, London, UK

Correspondence: Professor Richard Piercy, Comparative Neuromuscular Disease Laboratory, Royal Veterinary College, 4 Royal College Street, Camden, London, NW1 0TU, UK; rpiercy@rvc.ac.uk

Running Title: Species-specific consequences of an E40K missense mutation in SOD1

Non Standard Abbreviations

DM	Degenerative Myelopathy
FACS	Fluorescence-activated Cell Sorting
fALS	Familial Amyotrophic Lateral Sclerosis
HEK Cells	Human Embryonic Kidney Cells
Mut-D	Mutant dog K40 SOD1
Mut-H	Mutant horse E40 SOD1
RLN	Recurrent Laryngeal Neuropathy
ROS	Reactive Oxygen Species
SOD1	Superoxide Dismutase 1
WTD	Wild type dog E40 SOD1
WTH	Wild type horse K40 SOD1
$\Delta\Psi m$	Mitochondrial Membrane Potential

Abstract

A glutamic acid to lysine (E40K) residue substitution in superoxide dismutase 1 (SOD1) is associated with canine Degenerative Myelopathy: the only naturally occurring large animal model of Amyotrophic Lateral Sclerosis (ALS). The E40 residue is highly conserved across mammals, except the horse, which naturally carries the (dog mutant) K40 residue. Here we hypothesised that *in vitro* expression of mutant dog SOD1 would recapitulate features of human ALS (i.e. SOD1 protein aggregation, reduced cell viability, perturbations in mitochondrial morphology and membrane potential, reduced ATP production and increased superoxide ion levels) and that horses naturally carry an allele that makes them overly susceptible to neurodegenerative diseases.

As in human ALS, expression of mutant dog SOD1 was associated with statistically-significant increased cytoplasmic aggregate formation, raised superoxide ion levels (ROS) and altered mitochondrial morphology (increased length and branching (form factor)), when compared to wild-type dog SOD1-expressing cells ($p<0.05$). Similar deficits were not detected in cells expressing the equivalent horse SOD1 variant. Our data helps explain the ALS-associated cellular phenotype of dogs expressing the mutant SOD1 protein and reveals that species-specific sequence conservation does not necessarily predict pathogenicity. The work improves understanding of the aetiopathogenesis of dog canine Degenerative Myelopathy.

Key Words: superoxide dismutase 1, horse, dog, degenerative myelopathy, amyotrophic lateral sclerosis

Introduction

For over 20 years, scientists have known that mutations within the gene encoding superoxide dismutase 1 (SOD1) enzyme cause some familial forms of the human neurodegenerative disease, Amyotrophic Lateral Sclerosis (fALS) [1, 2]. SOD1 mutations were not known to be associated with any other naturally-occurring neurological diseases in mammals until 2009, when Awano *et al*. identified a significant association between a missense mutation in SOD1 – the substitution of a glutamic acid residue for a lysine residue at the 40th codon (E40K) – and the development of Degenerative Myelopathy (DM), an ALS-like disease of dogs [3]. Affected dogs are now used as a large animal model of ALS [4] since both ALS and DM share a key disease feature: the degeneration of long motor neurons [4, 5]. A protein's ability to cause disease can solely rest with expression of the mutant protein (complete penetrance) or its pathogenesis can be modified by other genetic or environmental factors [6]. The dog DM-associated SOD1 E40K mutation has autosomal recessive inheritance with incomplete penetrance [3]: variants in the SP110 gene, as well as aging, are the most important risk factors for disease development [7]. This means that dog E40K mutant SOD1, and other genetic variants contribute to the DM phenotype.

Horse SOD1 shares 75% amino acid identity to that of dogs, but notably, the lysine residue of mutant DM dogs occurs naturally in horses [8]; in contrast, in the vast majority of mammals sequenced (within the Ensembl database), the glutamic acid residue is conserved. Our pilot work (not shown) confirmed that the horse lysine residue at the 40th codon in SOD1, can be traced back at least as far as an ancestral horse genome derived from an animal from the middle of the Pleistocene age (4-4.5 million years ago) [9]. However, as ALS-like diseases, such as Equine Motor Neuron Disease and long motor nerve degeneration (e.g. as seen in Recurrent Laryngeal Neuropathy (RLN)) occur in horses - some with high prevalence [10, 11] - it seems reasonable to speculate that wild-type K40 horse SOD1 could predispose these animals to neurodegenerative diseases. Indeed, recent evolutionary pressures, such as domestication (2000-5000 years ago [12]) or modern management (such as lack of antioxidant provision [13]) - perhaps in combination with genetic modifiers - might contribute or be necessary for disease onset. Similar domestication and modern management-associated disease exacerbation occurs in another highly prevalent equine genetic neuromuscular disease [14-16]. If true for horse SOD1, this would shed significant light on the role that the enzyme and its associated pathways

play in mammalian neurophysiology and highlight the interaction between evolutionary biology and the modern environment and domestication.

The main function of SOD1 is to catalyse the first stage of the neutralisation of superoxide free radicals (O_2-) into hydrogen peroxide and molecular oxygen [1, 17, 18]; however, the mechanisms behind motor neuron degeneration in mutant animals have not been fully elucidated. Despite this, most authors agree that the neurodegeneration results from a toxic gain-of-function, rather than to a loss of enzymatic activity [19, 20]. The most common pathological feature reported with ALS- and DM-associated SOD1 mutations is aggregation of the mutant SOD1 protein, but these aggregates occur late in the disease course, so there is speculation over whether soluble toxic oligomers might convey earlier disease pathogenicity [1, 3]. A recent paper highlighted the importance of the residue at the 40th codon (and its molecular bonds with 91st codon) in human SOD1 in determining the correct structure of the enzyme, as substitution of the wild-type glutamic acid (E) residue to certain residues (aspartate (D), glycine (G), or valine (V)) introduced steric hindrance within the β-barrel plug, and increased protein accumulation [21]. Crisp *et al*. investigated the possible biochemical differences between the wild-type and mutant dog SOD1 revealing that the mutant enzyme has a greater propensity to aggregate, compared to the wild-type protein *in vitro*. These authors also reported normal enzymatic activity and dimerization of the mutant dog enzyme (SOD1 exists as a homodimer) likely because the 40th codon, (in Greek Key loop 3), is remote from the active site, metalation sites and structural dimerization bonds [3, 22]. Other common cellular perturbations seen in ALS-models include mitochondrial dysfunction and increased oxidative stress [23-25] but these (to date) have not been examined for the dog SOD1 mutation. Consequently, further details of the pathogenesis associated with the K40 mutation in dog SOD1 remain unknown, which limits appreciation of its importance as a naturally occurring ALS model.

The principal aim of our work was to investigate cellular perturbations associated with expression of the dog K40 SOD1 protein, and that similar perturbations may be seen with expression of the horse K40 SOD1 protein, making them potentially more susceptible to neurodegenerative disease.

Materials and Methods

SOD1 Genotyping in Different Perissodactyla Species and Horse Breeds

The Perissodactyla order contains 3 families: Equidae (including horse, zebra, donkey and ass), Rhinocerotidae and Tapiridae [158]. Exon 2 of SOD1 was amplified from DNA extracted from residual EDTA blood samples from different horse breeds (obtained with owner consent), Donkey (obtained from the Donkey Sanctuary), Przewalski's horse, Chapman's zebra, Onager and Malaysian Tapir (latterly all kindly provided by the London Zoological Society). Briefly, DNA was extracted from blood samples and amplified using a PCR reaction with species-specific primers, as described below (see Supplementary Table A), gel extracted and Sanger sequenced.

Plasmid Vectors

Dog and horse cDNA SOD1 cassettes were produced by PCR amplification of cDNA generated from mRNA derived from muscle, ensuring amplification of the initiation Kozak sequence to beyond the terminal stop codon in the full coding sequence. Dog cDNA was derived from a dog that was heterozygous for the E40K SOD1 mutation. Amplicons were cloned (pCR2.1topo; Invitrogen) and dog E40 (WTD) and K40 (Mut-D) and horse K40 (WTH) variants were selected. Thereafter, the horse K40 sequence was mutated (by PCR mutagenesis) to generate an E40 variant (Mut-H) (primer sequences listed in Supplementary A). All sequences were verified by Sanger sequencing. Each of the 2 variants, for each species were then cloned into a pLVX-EF1α-IRES-ZsGreen (Clontech, Saint-Germain-en-Laye, France; 631982), using Clontech In-Fusion methodology (HD Cloning Kit; Clontech, Saint-Germain-en-Laye, France; 639646). A vehicle control was produced that consisted of the plasmid without any SOD1 insert.

Lipofectamine Triple Transfection for Production of Lentiviruses

Each plasmid was transfected (Lipofectamine 2000, ThermoFisher Scientific, UK; 11668027) into HEK-293T cells, alongside 2nd generation packaging (PAX-2 (Addgene, Cambridge MA, USA; #35002)), and envelope (pMD2.G (Addgene, Cambridge MA, USA; #12259)) plasmids to produce lentiviral particles that were subsequently harvested [26]. The lentiviral particles were then resuspended in phosphate buffered saline (PBS) and the number of viral particles present per millilitre (transducing units per ml (TU/ml)) determined. Briefly, increasing dilutions of lentiviral particles were applied to HEK-293T cells, incubated for 24 hours and, using Fluorescent Analysis Cell Sorting (flow cytometry), GFP positive cells counted. A control

well was included for each different lentivirus, which was left untreated. Typically yields of $1x10^8$ TU/ml were achieved.

Cells analysed using a flow cytometer (FACS; BD FCSCanto), were gated according to forward and side scatter and 525nm and 575nm (red) when excited at 488nm. Cells were gated according to forward scatter and side scatter. A minimum of 10000 cells was counted per replicate per condition for each well for all experiments. Where it was necessary simultaneously to evaluate both the green and red fluorescence of individual cells, fluorescence compensation was used. Compensation settings remained constant throughout the entire experiment.

Cell Types and Cell Culture Conditions

Either HEK-293T cells (mitochondrial assays) or SHSY5Y cells (aggregation and viability assays) were used. Both cells were obtained from the European Collection of Cell Cultures (HEK-293T Catalogue Number 05030204 and SHSY5Y Catalogue number 94030304). All cells were incubated in Dulbecco's modified Eagle media (DMEM; Sigma, UK #D5546), with 10% heat-inactivated foetal calf serum (FCS) and 2mM (1%) L-glutamine and 1% penicillin (10IU/ml)/streptomycin (100µg/ml) (maintenance media) for 24 hours at 37°C 5% CO2, before being virally transduced with appropriate vehicle and untreated control wells. Viruses were added at a multiplicity of infection (MOI) of 20, and incubated for another 48 hours.

Transgene Expression

Following lentiviral transduction, expression of the different SOD1 variants at mRNA (SHSY5Y cells, n=3) and protein levels (HEK-293T and SHSY5Y cells, n=3), was performed by quantitative real-time PCR (qPCR) and western blot. Cells seeded at 100,000 cells per well in a 6 well plate, were cultured for 24 hours in maintenance media before adding lentiviruses expressing each of the 4 SOD1 variants and the empty (vehicle) vector to wells. One control well was left untreated. After 72 hours all RNA and proteins were extracted. The mRNA was extracted using RNA-Bee reagent (Amsbio) according to the manufacturer's protocol (with inclusion of an additional 1:1 chloroform extraction following phase separation, and inclusion of glycogen at 10µg/ml during precipitation to maximise RNA yield). Proteins were solubilised in 250µl of chilled radioimmunoprecipitation assay buffer (RIPA) (50mM Tris pH 7.5, 150mM NaCl, 1% NP40, 0.5% NaDeoxychlorate, 0.5% SDS, 1mM EDTA, 1mM EGTA, 1mM PMSF and 1x protease inhibitor), and cellular debris pelleted. Soluble proteins within the supernatant

were removed and quantified against known bovine serum albumin protein standards (BioRad DC Protein Assay, UK).

Equal protein sample concentrations were boiled, with a loading buffer, for 5 minutes, and proteins separated on a commercially-available precast polyacrylamide gel (Any kD Mini-PROTEAN TGX Stain-Free Gel, BioRad, UK; 4568123S) (100V for 90 minutes) and transferred (300mA for 90 minutes) to a PVDF blotting membrane (Amersham Hybond P, GE Healthcare Life Sciences. UK; RPN303D). Membranes were blocked in PBS with 0.05% Tween containing 10% milk powder for 1 hour at room temperature followed by incubation with an anti-SOD1 antibody (FL-154, sc-11407; Santa Cruz Animal Health at 1:1000) and an anti-beta-tubulin antibody (as a loading control) (ab6046, Abcam, UK, at 1:10000), in PBS with 0.05% Tween containing 5% milk overnight, at 4°C. Following 3 washes, secondary goat anti-rabbit-IgG horseradish peroxidase-linked whole antibody (Dako, UK; #D0487 at 1:5000) in PBS-0.05% Tween was added and incubated for 1 hour at room temperature, whilst shaking. Blots were developed with Amersham ECL Prime Western Blotting Detection reagent (GE Healthcare, UK; #RPN2232) and visualised on a Kodak developer. Blots were run on all biological replicates.

Quantitative PCR

All samples for comparison by qRT-PCR were processed together. qRT-PCR assays were designed to amplify species-specific regions of SOD1, including human, dog and horse to allow for quantification of their total expression in comparison with 3 housekeeping genes. These 3 housekeeping genes were GAPDH, POLR2F and MPRIP which have stable expression in SHSY5Y cells [27]. RNA quantity and purity were confirmed by Nanodrop analysis (ND1000, Thermo Scientific). A cDNA library was synthesised from the isolated RNA using the Precision nanoScript2 Reverse Transcriptase kit (Primerdesign). Random nonamer and oligo-dT priming were both used during this cDNA synthesis stage with 1.6µg of total RNA per 20µl reaction. Following synthesis, cDNA samples were diluted (1:10) with RNAse/DNAse-free water, giving a final cDNA concentration of approximately 4ng/µl (assuming 1:1 conversion of RNA to cDNA).

qPCR reactions were performed in triplicate with 2µl cDNA per well (approximately 8ng), using PrecisionPLUS SYBR green Mastermix (Primerdesign). The primers were used (Supplementary Data A) at a final concentration of 500nM. Primers for the housekeeping genes

were sourced from Hoerndli FJ *et al*. 2004 [27]. Reactions were run on a real-time-PCR light cycler (CFX384 light cycler; BioRad), in black 96-well plates, with clear caps (ThermoScientific). All runs included melt curve analysis and template-free controls. All primer pairs produced single amplicons and reactions were of comparable efficiency (95-100%) as established by standard dilution curves and analysis of individual traces. The qPCR cycle used was as previously reported [28, 29]. Quantification cycle (Cq) values were determined by regression analysis of the amplification traces. Average Cq values for each replicate reaction were used directly before analysis (Normfinder, geNorm). Samples exhibiting more than 10-fold deviation in relative expression from the dataset average in a majority of genes were typically excluded from analysis. Experimental normalisations using suitable candidates used the linearised expression data of the respective genes, or where multiple normalisation genes were used, the geometric average of the linearised expression data.

Aggregation Studies

Cells were seeded onto glass coverslips pre-treated with Matrigel (BD Matrigel, BD Biosciences, UK; 1:10) at a density of 50000 cells per coverslip in 24 well plates. Cells on coverslips were infected in triplicate, on 3 different occasions (n=9). Forty-eight hours after transduction all coverslips were washed with PBS, fixed (4% paraformaldehyde (PFA)/0.1% triton; 4°C for 20min, followed by 8% PFA; 30min at room temperature) and stained with a nuclear marker, Hoechst (Life Technologies, UK; at 1:5000, in PBS). All cells were immunolabelled for SOD1 (0.1% triton in PBS for 30 minutes at room temperature, wash step, using an anti-SOD1 antibody (FL-154, Santa Cruz) 1:100 in PBS for 1 hour at room temperature, wash step, and lastly addition of a secondary antibody bound to the AlexaFluor 594, 1:500, 1 hour at room temperature). The coverslips were mounted onto glass slides using Hydromount (National Diagnostics, UK; HS106). Each slide, containing all replicates from one condition, was examined with the investigator blinded to the condition, using fluorescence microscopy, and 10-15 random images were captured (using 40x objective) per coverslip. The total number of transduced (green) cells was recorded per image, and of these, the total number of cells containing cytoplasmic, nuclear or cytoplasmic and nuclear aggregates recorded. Aggregates were defined as intense accumulations of red colouration either within the cytoplasm or nucleus of a cell [19]. The results per image were summated for each of the 9 replicates per condition.

Viability

SHSY5Y cells were plated at a density of 50000 cells per well in maintenance media and viral transduction performed after 24 hours. After another 48 hours H_2O_2, at concentrations ranging from 0, 200, 400, 600, 800 and 1000μM in maintenance media, were added to each condition, in triplicate. The cells were incubated in H_2O_2 for exactly 24 hours before being trypsinised, pelleted, washed in PBS and stored on ice for no longer than 30 minutes. Any floating cells were collected and added to the trypsinised cells before pelleting. To quantify how many cells had died, the cell pellets were resuspended in propidium iodide (1mg/ml in water; Sigma-Aldrich, Gillingham, Dorset UK) (1:500 dilution in PBS), incubated for 1 minute, at room temperature in the dark and then the number of red cells were recorded by flow cytometry. Untreated control cells set the background redness levels.

Mitochondrial Assays

Mitochondrial Morphology and Volume

HEK-293T cells were seeded at a density of 25000 cells per chamber in a 35mm glass-bottomed, imaging dish with 4 compartments (u-Dish 35mm Quad ibiTreat, ibidi, Germany). Each condition had 4 replicates. Forty-eight hours after viral transduction the media was removed, and the cells incubated at 37°C for 30-45 minutes with 250μl of recording media (125mM NaCl, 5mM KCl, 1mM NaH2PO4, 20mM HEPES, 5.5mM D+ glucose, 5mM NaHCO3, 1mM CaCl2, pH 7.4) containing 50nM MitoTracker Red FM (Molecular ProbesTM, Thermo Fisher Scientific, M22425). Five minutes before imaging, 1μl of the nuclear marker Hoechst 33342 was added to the well. Control cells were incubated with magnesium green (Thermo Fisher Scientific, M3733) (4μM in the recording media, containing the MitoTracker Red). Z-stacks were acquired using a Leica SP5 confocal microscope (63X objective) on a randomly-selected region of >10 transduced cells. The number of slices and step size were kept constant, and the microscope detection settings were fixed.

The shape descriptors aspect ratio (AR) and form factor (FF) were evaluated as measures of mitochondrial elongation and branching, respectively. The z-stacks were imported into ImageJ (Fiji; [30]). Here, the image within the z-stack that was most representative of the mitochondrial network in a transduced cell was selected, and thresholding performed (settings were kept constant across all replicates). The cell was highlighted and the AR and FF (1/circularity) calculated. This was repeated for every transduced cell imaged (minimum of 10 cells per replicate, four replicates per condition).

To assess mitochondrial volume, analysis was performed using the Volocity software, where a custom package was designed to allow for the calculation of the cytosolic volume (green), the nuclear volume (blue) and the mitochondrial volume (red).

Mitochondrial Membrane Potential (Δψm)

Confocal Microscopy: Experimental conditions were set up as described above for the mitochondrial morphology and volume experiments. Continuous monitoring of Δψm was achieved by loading HEK 293T cells with the fluorescent potentiometric dye TMRM (Sigma, T5428). A non-quenching concentration of TMRM (50nM) in recording media supplemented with 10μM verapamil hydrochloride (Sigma, V4629) was added to all wells. The cells were incubated for 30 minutes at 37°C. Real-time imaging was performed on a temperature-controlled (37°C) Leica SP5 confocal microscope (40X objective). Time series were acquired and the mitochondrial TMRM fluorescence decay was monitored in real-time, until a plateau was reached. At this point, directional dye behaviour was confirmed by adding 20nM carbonyl cyanide 4-(trifluoromethoxy) phenylhydrazone (FCCP; Sigma Aldrich C2920). Time series were analysed using ImageJ (Fiji; [30]). Settings were kept constant throughout all experiments.

Flow Cytometry: HEK-293T cells were seeded at a density of 25000 cells per well in a 24 well plate and incubated in maintenance media for 24 hours, at 37°C 5% CO_2, followed by viral transduction. Cells were trypsinised, the cell suspensions pelleted by centrifugation and the supernatant discarded. The cells were then resuspended in recording media containing 50nM TMRM and incubated for 30 minutes at 37°C, before they were repelleted by centrifugation and the supernatant replaced with PBS. The cell pellets were kept in the dark on ice, for no more than 30 minutes, while the red intensity of transduced cells was recorded using a flow cytometer. Correct directional dye behaviour for TMRM was confirmed for all conditions (vehicle, WTD, Mut-D, WTH and Mut-H) and control cells (non-virally transduced cells) using 20nM FCCP. Each condition was plated out in triplicate and this experiment was repeated on three occasions: (i.e. n=9 per condition).

ATP production

ATP production was measured across all conditions and untreated HEK-293T control cells, using a commercially-available colourimetric assay (ATP Assay Kit (Colourimetric/Fluorometric), Abcam, ab83355). Transduction efficiencies were confirmed to be >97% (via flow cytometry) for all conditions. HEK-293T cells were plated out at 500000

cells per well (6-well plate), and virally transduced. Four replicates were included per condition. Forty-eight hours after transduction the cells were trypsinised and counted using a haemocytometer. All cell suspensions were diluted to 500000 cells per 50µl with an ATP Assay Buffer (supplied with the kit). ATP concentrations were determined according to the manufacturer's protocol, in duplicate, with appropriate background controls included per replicate. A standard curve from known ATP concentrations (0-10nmol) was included for each plate that was read. The optical density at 570nm was read using a microplate reader (SpectraMax L Luminescence Microplate Reader, Molecular Devices). All duplicate readings were averaged (for standards and samples), and the background control readings subtracted. The corrected absorbance values for the standard ATP concentrations were plotted and a line of best fit drawn.

Superoxide production

Flow cytometry was utilised to measure the red fluorescence of the virally-transduced cells when treated with the MitoSOX™ Red reagent (Thermo Fisher Scientific, M36008). HEK-293T cells were plated out at 50000 cells per well, in a 24 well plate. Conditions were set up in triplicate, and the experiment was repeated on 3 separate days (n=9 total). Forty-eight hours after viral transduction, wells were washed with PBS, trypsinised, the cells pelleted and stored on ice for no more than 30 minutes. Cells were resuspended in 5µM MitoSOX Red in PBS and incubated at 37°C for 10 minutes. Red fluorescence intensities were assessed in a minimum of 10000 virally-transduced cells per replicate, per condition, via flow cytometry. The median red fluorescence intensity was averaged across each replicate per condition as a measure of the levels of superoxide ions as it was not possible to assess whether the data was normally distributed.

Protein Charge

The change in the net charge, at physiological pH, between the wild-type and mutant forms of dog and horse SOD1 variants was calculated using commercially-available software, Innovagen [31].

Statistics

Continuous data were analysed with either a one-way (aggregation) or two-way (viability) ANOVA and post-hoc testing consisted of Tukey's multiple comparison test. Differences were considered statistically significant when $p<0.05$. To account for the effects of replicate

(mitochondrial morphology and membrane potential (confocal microscopy)) or day (mitochondrial membrane potential (FACS), ATP and superoxide levels) on the results achieved, linear regression using the following equation was used: outcome ~ SOD1 genotype + effect (i.e. day or replicate). Post-hoc testing (Tukey's multiple comparisons test) was performed to assess if there were any statistically significant differences ($p<0.05$) in the outcome, across the different SOD1 variants.

Results

Perissodactylae SOD1 Genotype

Sequencing of the equid species (including 7 different horse breeds (Supplementary Data B), donkey, zebra, onager and Przewalski's horse) and the Tapiridae (Malaysian Tapir) revealed conservation of the lysine (K) residue in all these species. In contrast, the onager was heterozygous at the 40^{th} codon, whereby an arginine (R) residue was also present (Figures 1 and 2).

Transgene Production

Successful transduction of all 4 SOD1 variants was confirmed by western blot analysis. The WTH and Mut-H SOD1 protein levels were consistently comparable in both HEK-293T and SHSY5Y cells (Figure 3B), however the WTD protein levels were consistently double those of the Mut-D SOD1 protein (Figure 3a). Correspondingly, the relative mRNA expression of WTD SOD1 was confirmed by qPCR, to be approximately double that of the Mut-D ($p<0.0001$) (Figure 3c), conversely no difference in the mRNA expression level of the WTH and Mut-H SOD1 was identified ($P > .05$) (Supplementary Figure 3).

Aggregation

Aggregation of mutant SOD1 proteins is a hallmark of both SOD1-associated human and canine diseases: ALS and DM [1, 31]. However, neither horse SOD1 variant showed an increased propensity to aggregate; conversely, as expected, the mean percentage of cells expressing the Mut-D SOD1 that contained cytoplasmic aggregates was significantly higher than the mean percentage of cytoplasmic aggregates in cells expressing all other SOD1 variants, and control and vehicle cells (Figure 4A and B).

Viability

Increases in cellular hydrogen peroxide will trigger cell death by apoptosis, once a threshold level is reached. We hypothesized that cells expressing either K40 SOD1 variants would be more susceptible to H_2O_2-induced cell death compared to their E40 counterparts. This hypothesis was rejected: cells expressing WTH or Mut-H SOD1 showed no significant differences in H_2O_2-induced cell death over the range of H_2O_2 concentrations applied (0-1000μM). Cells expressing WTD SOD1 had similar susceptibility to H_2O_2-induced cell death as cells expressing Mut-D SOD1 over the entire range of H_2O_2 concentrations applied (0-1000μM) ($p>0.05$) (Figure 5 A-F).

Mitochondrial Morphology

A cell's mitochondrial network is a complex, often highly branched system kept in a careful balance between fission and fusion. Imbalances in their morphology can reflect impaired functionality and are reported in ALS-models [25]. There were no differences in the morphology of the mitochondrial networks in cells expressing the WTH and Mut-H SOD1 variants and there were no statistically significant differences between the cells expressing the dog SOD1 variants evaluating the Aspect Ratio. However, the form factor (branching) was significantly greater in cells expressing the Mut-D SOD1 protein compared to cells expressing the wild-type dog SOD1 ($p<0.05$) (Figure 6). There were no significant differences noted between the mitochondrial volumes of transduced HEK-293T cells under any of the conditions (control, vehicle or SOD1 variants) ($p>0.05$) (Supplementary Figure 2).

Mitochondrial Membrane Potential

As recommended by Perry *et al*. 2011, two methods were used for measurement of the $\Delta\Psi m$ [33]. However, there were no statistically significant differences in the $\Delta\Psi m$ between any of the SOD1 variants, identified using confocal microscopy (Figure 7A) or flow cytometry (Figure 7B). Cells expressing the mutant dog SOD1 (5028 ± 6716) produced significantly greater levels of superoxide ions compared to all other SOD1 variants and controls (control 373.6 ± 168.4 $p=0.0008$, vehicle 427.2 ± 252.5 $p=0.0009$, WTD 870.2 ± 950.5 $p=0.002$ WTH 1784 ± 1629 $p=0.016$ and Mut-H 1362 ± 521.5 $p=0.012$), however no $\Delta\Psi m$ (either measured with flow cytometry or confocal microscopy) (or ATP level differences) were seen between them and the wild-type dog SOD1 expressing cells.

ATP Production

The mean ATP concentrations (nmol/5x10^5 cells) were lower for the K40 SOD1 variants for both dog and horse, with the Mut-H-SOD1-expressing cells having a statistically significant higher mean ATP concentration than the 2 K40 SOD1 variants ($p<0.05$) (Figure 7C).

Superoxide Ion Concentrations

Superoxide ions are mainly produced by complex I and III of the electron transport chain and are deposited in the intermembrane space within mitochondria [34]. Elevations of these reactive oxygen species (ROS) are a common feature of different ALS-causing SOD1 mutations and are particularly deleterious to many cellular structures and functions [23]. In the cells expressing the Mut-D SOD1 variant, the superoxide concentrations were significantly higher than all other conditions ($P<0.05$) (Figure 7D).

Protein Charge

The substitution of a glutamic acid for a lysine residue in SOD1 was predicted to result in the net charge (at pH 7.4), to change by +2 [31]. This would change the overall charge of the dog K40 SOD1 to -1.4 (mutant) from -3.4 (wild-type). The overall charge of the wild-type horse SOD1 was lower than the charges of the different dog SOD1 variants at -4.2 (and hence the mutant horse variant was predicted to have charge, -2.2).

Discussion

This research was aimed at further investigating the cellular consequences of a mutation in dog SOD1 associated with an ALS-like phenotype and examined whether similar perturbations exist when associated with the equivalent horse protein. We identified prominent cellular deficits in cells expressing dog mutant SOD1 including raised superoxide ion concentrations and altered mitochondrial morphology; as such, our work further corroborates the work of Crisp *et al.* [19], and reveals additional functional deficits associated with the dog DM mutation that relate closely to those detected in SOD1-associated ALS [23, 25]. In contrast, our work shows that a lysine residue at the 40th codon in horse SOD1 does not produce the same pathological phenotype *in vitro*. Previous analysis of the biochemistry of the mutant dog SOD1 protein did so using a fluorescent protein-tagged mutant dog SOD1, however fluorescent tagging of SOD1 proteins can alter their biochemical properties [19, 35, 36]. Instead, here we examined aggregation tendency using an untagged approach. Our work confirms that the mutant lysine residue at the 40th codon in dog SOD1 background induces protein aggregation.

The 40th codon in SOD1 is located between the 3rd and 4th β strands in Greek key loop 3 and the pathogenicity of mutations in this region. has recently been speculated to arise from the introduction of steric hindrance, caused by opposing charges or side-chain repulsions, resulting in loss of the β-barrel plug (which maintains hydrophobicity in the core of the SOD1 molecule) and thus promoting SOD1 protein misfolding and aggregation [21]. In humans, an E40G mutation is reported to be associated with development of fALS [37], however, mutating the 40th codon to a lysine (K) residue in humans did not increase the human SOD1's propensity to aggregate [19], similar to our results for the wild-type horse SOD1. This implies that other residues in the dog SOD1 protein act with the K40 amino acid to produce the mutant dog SOD1's deleterious aggregation. This phenomenon has been reported previously 38-40; for example, in 1997 the first causative mutation of Parkinson's disease in alpha-synuclein (A53T) was published, in contrast, the mutant residue T53, is the wild-type residue in rodents.40 Parkinsonian-like diseases are not reported to occur spontaneously in rodents [41], suggesting that the presence of threonine in rodent alpha-synuclein is non-pathogenic in contrast to humans. These species specificities might therefore explain the common occurrence of failure of artificially generated (predominantly) rodent models to recreate the human phenotype: even recently, several devastating mutations within the human α-sarcoglycan gene, when created in the equivalent mouse gene, failed to produce a dystrophic phenotype [38]. Our study therefore is an important reminder that protein sequence differences between species can affect a missense mutation's pathogenicity. It also supports the use of naturally-occurring (spontaneous) animal models (i.e. with pre-identified relevant phenotypes) in disease investigation.

The propensity of ALS-associated SOD1 mutants to aggregate is influenced by several factors [21, 42-46] which collectively affect the protein's stability immediately after its biosynthesis; decreased stability increases protein aggregation [47]. The protein's charge at a physiological pH being more negative can convey a greater stability [47-50]. Thus the more negative charge of the horse K40 wild-type SOD1 (−4.2) (compared to K40 mutant dog SOD1 with an overall charge of −1.4) could make it inherently more stable and, presumably therefore, less likely to aggregate. Interestingly, in human SOD1 the residue present at the 40th codon is pivotal for correct folding of the protein, and as such to resist protein aggregation [21], perhaps by maintainance of the hydrophobic center of the enzyme. Although the human K40 SOD1 has not been shown to have an increased aggregation potential [19], their G40 (ALS-causing SOD1 mutation), D40, and V40 (tagged to YFP) counterparts appear to form increased numbers of

fluorescent inclusions in a cell-based model as well as being predicted in silico to hinder appropriate intramolecular bonds [21]. The residue at the 40th codon forms the hydrophobic barrier (β-barrel plug) in partnership with the 91st codon equivalent, being in humans (and dogs) typically K(91), whereas in horses it is an E. The latter suggests that in the wild-type horse SOD1 the K40 and E91 have effectively reversed, presumably still producing an efficient β-barrel plug. Thus it could seem surprising that the mutant horse SOD1 (E40) protein here did not show an increased propensity to aggregate however, the situation is likely more complex, probably affected by the surrounding residues as the human K40K91 SOD1 variant also did not show an increased aggregation [19]. Future work to investigate if these surrounding residues moderate any negative effects the 40th codon residue may have on aggregation, within the dog and horse SOD1 proteins seems important.

The lysine residue at the 40th codon is conserved across 5 different species within the Perissodactyla order, with the exception of the Onager whereby the individual was heterozygous for the lysine (K40) residue and an arginine (R40) residue. We also confirmed that the K40 horse SOD1 variant was present in an equine ancestor, 4-4.5 million years ago by blasting the *SOD1* exon 2 sequence of the modern horse genome to the ancient horse genome [9], and it appears that evolutionary pressures have not resulted in the removal of this residue; to the best of the author's knowledge there is no publically available horse genomes where a different residue can be found at the 40th codon, and within our laboratory we have identified this residue at the 40th codon in over seven different horse breeds (Supplementary Figure 1). Such pressures could have included domestication, whereby horses were selectively bred for their coat-colour, greater height and lower limb sturdiness [12]; greater height is the principal risk factor for the development of RLN in horses (an ALS-like long-motor axonopathy). Indeed in dogs, to develop the DM phenotype, advancing age as well as the expression of the K40 SOD1 protein is typically needed [3], highlighting that the K40 residue might only be pathogenic under certain circumstances. Certain circumstances might simply have not developed or been applied to horses to allow for manifestation of a pathological phenotype. Alternatively, we cannot rule out the possibility that other (as yet unidentified) deficits associated with the K40 horse protein, might predispose to neurodegeneration in (for example) especially long axons, as seen in equine RLN [11].

An important pathological feature of ALS-models is higher cellular ROS levels in cells expressing mutant SOD1 variants [23]. Superoxide ions (in particular) are highly reactive and

severely deleterious to cells, causing damage to DNA and lipid membranes. Thus, the fact that superoxide concentrations were significantly higher in cells overexpressing the mutant dog SOD1 compared to all other SOD1 variants, and controls, reveals an important feature underlying DM in dogs. Possible pathophysiological mechanisms underlying these higher superoxide levels include (i) activation of cytochrome c-catalysed oxidation and peroxide production causing elevated ROS levels (as seen when mutant G93A human SOD1 accumulates within the mitochondrial intermembrane space) [51], (ii) complex 1 inhibition (see below) and (iii) a reduction in the enzymatic activity of mutant SOD1 proteins. Saccon *et al*. 2013 showed that even mutant SOD1 proteins with mutations remote to the protein's active site can have reduced dismutase activity, likely due to disruptions with SOD1 binding to important co-factors [20]. An E40K dog SOD1 recombinant protein had normal enzymatic activity [19], however the activity of the endogenous mutant protein has not been evaluated. Further work is needed fully to tease out the mechanism(s) underlying the elevation in superoxide levels seen with K40 dog SOD1 expressing cells; however, our data reveals the possible role of treatments aimed at quenching free radicals in treatments of affected dogs (and humans with ALS).

Mitochondrial morphological perturbation in cells expressing the mutant dog SOD1 variant was revealed in this model: the mean form factor of mutant dog SOD1 expressing cells was significantly greater than the mean form factor of wild-type dog SOD1 expressing cells. Form factor describes the degree of branching of a cell's mitochondrial network and when evaluating the mitochondrial networks, qualitatively, in cells expressing the mutant dog SOD1 the increased form factor appeared to be characterised by an increased interconnectivity of the mitochondria (rather than an absolute elongation). This could result from increased fusion of neighbouring mitochondrial, coupled with decreased mitophagy. Increased form factor occurs in cells expressing mutant Parkin in an *in vitro* model of Parkinson's Disease [52], in cells transiently treated with rotenone [53] and when cellular ROS levels are elevated [54]. Certain Parkin mutations reduce the activity of complex I within the electron transport chain, and as rotenone is known to be an inhibitor of complex I [52, 55], it seems reasonable to assume that impairment of complex I leads to increased mitochondrial branching. In addition, various human mutant SOD1 proteins also reduce the activity of complex 1 [56, 57]. This could suggest that the increased form factor seen in cells expressing the mutant dog SOD1 protein results from the mutant protein's interaction with complex 1 and inhibiting its activity. Indeed, this inhibition can lead to elevated superoxide levels (as seen here), and reduced ATP production.

(ATP levels were lower in cells expressing the mutant dog SOD1 compared to the wild-type dog SOD1, although not significantly) [58, 59]. Future work investigating imbalances between mitochondrial fusion and fission, and the role of ROS in dog DM and ALS [60] seems important.

We found no difference in the inner mitochondrial membrane potential ($\Delta\Psi m$) of cells expressing the different SOD1 variants. However, since mitochondrial dysfunction was identified in other ways, it is conceivable that a longer expression time course might be needed to fully elucidate the affects of mutant dog SOD1 on $\Delta\Psi m$ (age is an important risk factor in ALS and DM) [61]. In contrast, human mutant G93A SOD1 reduces the $\Delta\Psi m$ within transfected NSC-34 cells [24], however this is one of the more severe SOD1 mutations encountered in human ALS [62]. Certain mitochondrial pathological phenotypes seen with the expression of SOD1 mutants only occur in neuronal cell lines [63], thus the measurement of the $\Delta\Psi m$ with mutant dog SOD1 expression might have been better investigated in a neuronal cell line. Alternatively, given that dog DM is recessive, the mutant proteins might need to be expressed on a SOD1-null background to detect $\Delta\Psi m$ defects.

Direct cytotoxicity and increased susceptibility to oxidative stress are both features seen with the over-expression of human SOD1 mutants in cell models of ALS [23, 24]. Conversely here the proportion of cell death induced by rising H_2O_2 concentrations was similar between the cells expressing the wild-type and mutant dog SOD1 proteins. The difference in cell viability is likely explained by several factors: the effect that different cellular backgrounds can have, the assay used to estimate viability and, most importantly, how deleterious the particular mutation is *in vivo*. The severity of ALS caused by human mutant SOD1 variants is directly associated with their ability to form aggregates [62]. Whilst the K40 mutation in dogs is associated with aggregation, aggregation is still relatively low in this model (mean percentage of cells containing mutant dog SOD1 aggregates: YFP-tagged mutant dog SOD1: approximately 20% [19] and non-tagged: 5.4%$\pm$1.8).

Mitochondrial abnormalities were not recorded in any of the assays performed with the wild-type or mutant horse SOD1 variants, therefore it was surprising to see a significant increase in ATP production in cells expressing the mutant horse (E40) SOD1 variant compared to the wild-type horse (K40) SOD1. Indeed, both species' K40 SOD1 variants-expressing cells had lower mean ATP levels, compared with their E40 SOD1 variant counterparts. Whilst we did not

identify ALS-associated cellular perturbations associated with the K40 SOD1 sequence of the wild-type horse SOD1, evolutionary change from E40 to K40 that occurred in horses, might have been at the expense of cellular ATP production, necessitating other concomitant evolutionary changes that now give horses their incredible oxidative capacity [64].

The validation of protein expression, following viral transduction with the dog SOD1 variants, consistently revealed lower mutant protein expression, in both HEK-293T cells and SHSY5Y cells. This phenomenon has been reported with dog and human SOD1 mutants in transfection and transduction experiments *in vitro* [23, 35, 62, 63, 65 with most authors commenting that the difference is solely explained by insoluble mutant SOD1 protein aggregates not being represented on a Western Blot [66]. However, the mRNA expression of various human mutant SOD1 have also been shown consistently to be lower than those of the wild-type SOD1 in an NSC-34 cell model of ALS [67] revealing other possible mechanisms. Ge *et al*. 2006 showed that mRNA of human mutant SOD1 variants G93A, A4V and G41S decayed at a significantly greater rate in transfected cells compared to the wild-type SOD1 variant [67], and this in turn was associated with decreased mutant SOD1 protein expression. The increased mutant SOD1 mRNA degradation, confirmed to be neuronal tissue specific, was accompanied by a loss of binding of the mutant mRNA to RNA-binding proteins, though the precise RNA binding proteins (there are over 420 known) were not identified [68]. The role of these pathways however is emphasised by the identification of implicated proteins in fALS (e.g. TDP-43) [73], as unbound RNP complexes can disrupt other cellular pathways [70]. Our data suggest that these pathways might also contribute to the dog DM phenotype.

In conclusion, here we thoroughly investigated cellular perturbations associated with a dog SOD1 mutation and examined its consequence in horses. Our study supports previous work into the pathological features associated with mutant dog SOD1, and importantly, extends this work to show that the endogenous (i.e. untagged) mutant dog SOD1 has a greater aggregation potential compared to its wild-type counterpart, and causes increased superoxide levels and an imbalance in mitochondrial fusion and fission. Further work is needed to fully investigate how expression of the mutant dog SOD1 perturbs cellular health in a more chronic disease model.

Acknowledgements:

This work was supported financially by the Horseracing Betting Levy Board (RS251) and conducted with ethical approval from the Clinical Research Ethics Review Board (2015 1381) of the Royal Veterinary College, University of London. No conflicts of interest are declared. The manuscript was approved by the Royal Veterinary College's research office and assigned CSS_02004.

Author Contributions:

All authors contributed to the experimental design. A. Draper, Z Wilson, C. Maile and D. Faccenda performed the experiments and analyzed the data; A. Draper and R. Piercy prepared the manuscript which was approved by all authors.

Figures

Figure 1. Conservation of the 40th codon in SOD1 across different mammalian species. A glutamic acid residue (E) is present at the 40th codon (blue) in most mammals with the exception of the wild-type horse, armadillo and the mutant SOD1 variant of the dog where a lysine (K) residue (red) is found.

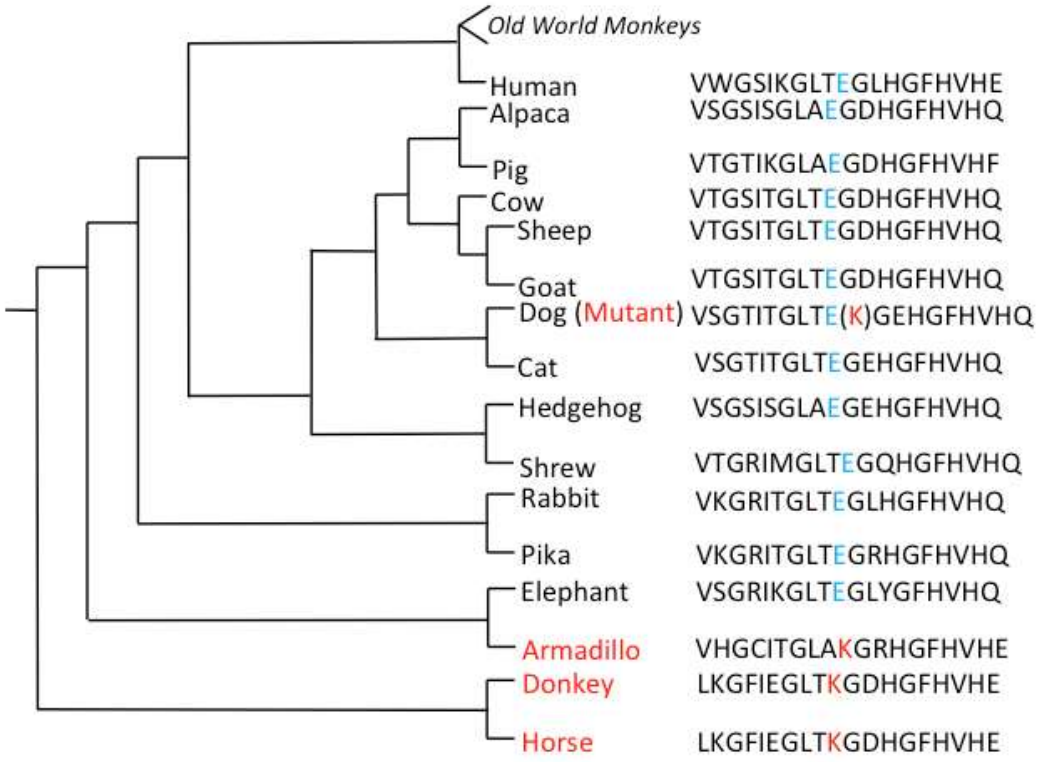

Figure 2 Genomic sequencing from five different Perissodactyla species (Horse, Przewalski's horse, Onager, Zebra, Donkey and Tapir), revealed conservation of the lysine residue at the 40th codon in all species with the exception of the Onager whereby the animal was heterozygous for an arginine residue (and lysine residue).

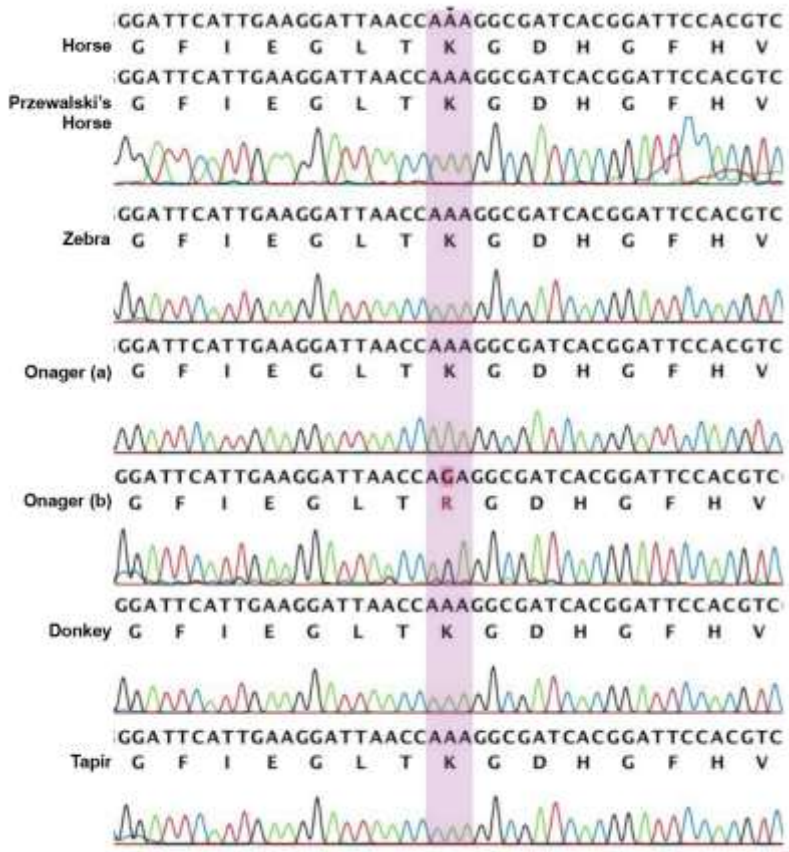

Figure 3 Western blot of exogenous SOD1 protein expression with the different variants. Equivalent protein expression of horse SOD1 variants (wild-type (K40) (WTH) and mutant (E40) (Mut-H)) were seen in virally-transduced cells (A). Whilst wild-type (E40) dog SOD1 mRNA (C) and protein (B) levels were approximately double those of its mutant dog (K40) SOD1 counterpart. Representative western blots from virally transduced cells expressing different SOD1 variants and blotted for SOD1 and β-tubulin (B-tub: loading control). Human and horse SOD1 separate at the same molecular weight (~18kD) whilst dog (dog) SOD1 (cSOD1) has a molecular weight of approximately 16kD.

A) Key: 1) control cells (no transduction), 2) vehicle alone, 3) wild-type horse (WTH) and 4) mutant horse (Mut-H).

B) Key: A) control cells, (no transduction), B) vehicle alone, C) wild-type dog (WTD) and D) mutant dog (Mut-D).

C) Relative expression of dog SOD1 (WTD (E40) and Mut-D (K40)) mRNA in virally transduced SHSY5Y cells, normalised to GADPH, MPRIP and POLR2F expression identified with specific primers to dog SOD1. The relative expression of WTD SOD1 was significantly greater than its Mut-D SOD1 counterpart ($p<0.0001$), in virally transduced cells. Negligible expression of dog SOD1 was seen in control and vehicle. Data is expressed as the mean $\pm$ standard deviation from experimental replicates (n=3). Bars represent the p-values (solid: $p<0.05$, dashed: $p<0.0001$) generated from One-way ANOVA statistical analysis with post-hoc testing.

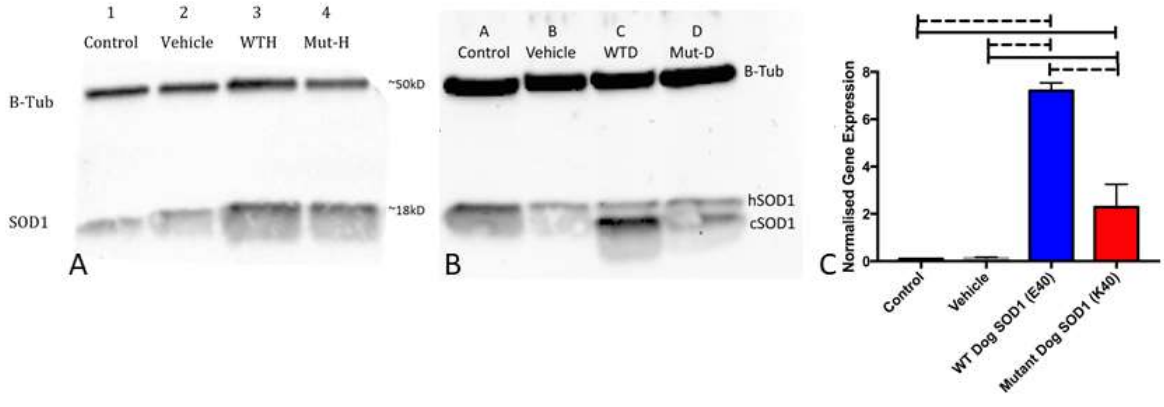

Figure 4 A, SOD1 immunocytochemistry of control and virally-transduced SHSY5Y cells including the vehicle (plasmid alone, no SOD1 insert), wild-type dog (E40) SOD1 (WTD SOD1), mutant dog (K40) SOD1 (Mut-D SOD1), wild-type horse (K40) SOD1 (WTH SOD1) and mutant horse (E40) SOD1 (Mut-H SOD1). Mutant dog SOD1 aggregates can clearly be seen (white arrow) and are noticeably absent from the other conditions. In the merged image nuclei fluoresce blue, positively transduced cells green (with the exception of the control cells) and SOD1 fluoresce red with immunolabelling. Black scale bar = 20μm. B, Graphical representation of the percentage of cells containing cytoplasmic SOD1 positive aggregates (identified by immunocytochemistry), with different dog and horse SOD1 variants (mean ± standard deviation). The cells expressing the mutant dog SOD1 protein contained significantly more cytoplasmic aggregates than compared to the other SOD1 variants and controls ($P < .05$). Different letters indicate statistically significant differences between groups ($P < .05$)

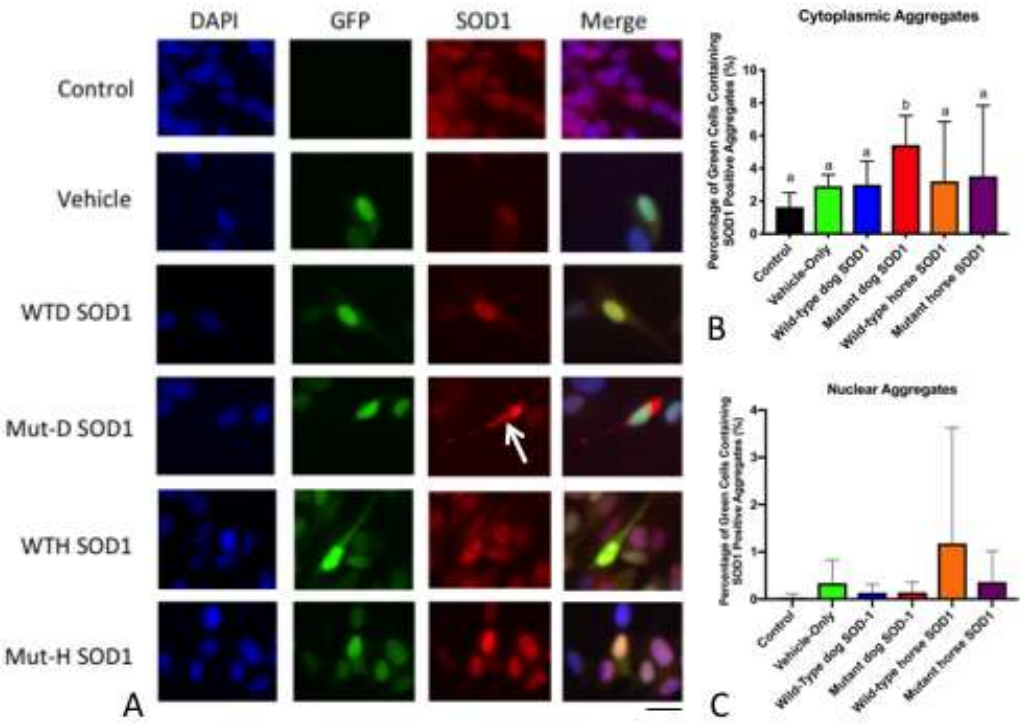

Figure 5 Susceptibility of SHSY5Y cells to H_2O_2-induced cell death over a range of H_2O_2 concentrations (0-1000μM), expressing different SOD1 variants via viral transduction (wild-type dog (E40) (WTD), mutant dog (K40) (Mut-D), wild-type horse (K40) (WTH) and mutant horse (E40) (Mut-H) SOD1), with control cells and a vehicle control (GFP-only). The mean percentage of dead cells (± standard deviation (error bars)) (as denoted by being propidium iodide (PI) positive on flow cytometry) is reported, for each condition, at specific H_2O_2 concentrations in panels b-f. P-values from Two-Way ANOVA with post hoc correction (Tukey's Multiple Comparisons Test) are reported.

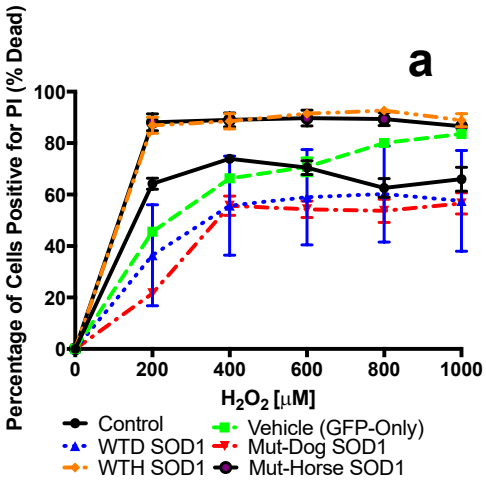
a
Percentage of Cells Positive for PI (% Dead)
100
80
60
40
20
0
0
200
400
600
800
1000
H2O2 [μM]
Control
WTD SOD1
WTH SOD1
Vehicle (GFP-Only)
Mut-Dog SOD1
Mut-Horse SOD1

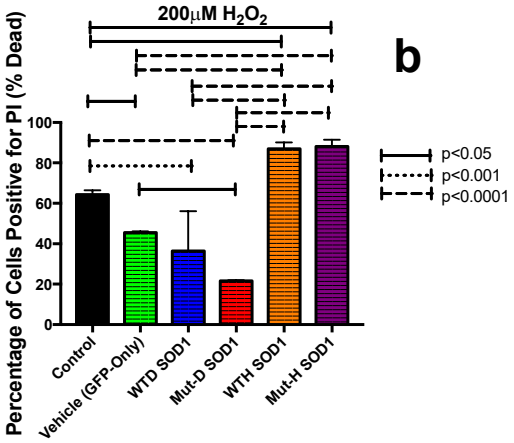
200μM H2O2
b
Percentage of Cells Positive for PI (% Dead)
100
80
60
40
20
0
Control
Vehicle (GFP-Only)
WTD SOD1
Mut-D SOD1
WTH SOD1
Mut-H SOD1
p<0.05
p<0.001
p<0.0001

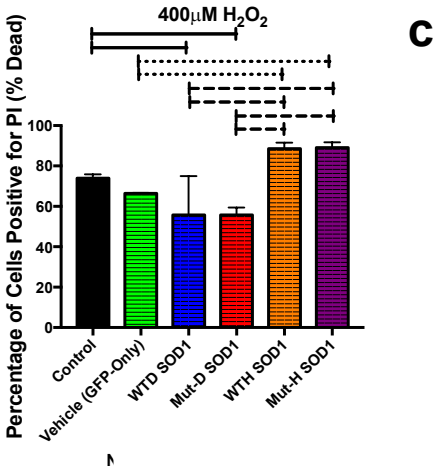
400μM H2O2
c
Percentage of Cells Positive for PI (% Dead)
100
80
60
40
20
0
Control
Vehicle (GFP-Only)
WTD SOD1
Mut-D SOD1
WTH SOD1
Mut-H SOD1

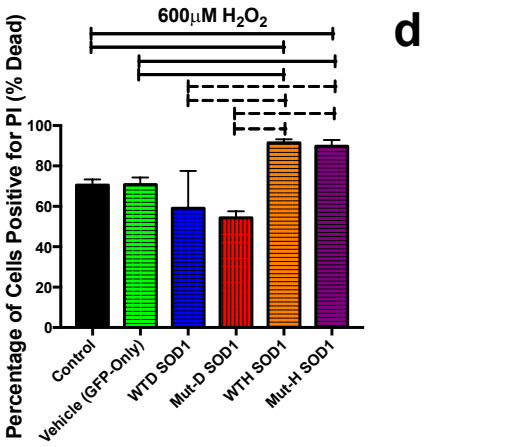
600μM H2O2
d
Percentage of Cells Positive for PI (% Dead)
100
80
60
40
20
0
Control
Vehicle (GFP-Only)
WTD SOD1
Mut-D SOD1
WTH SOD1
Mut-H SOD1

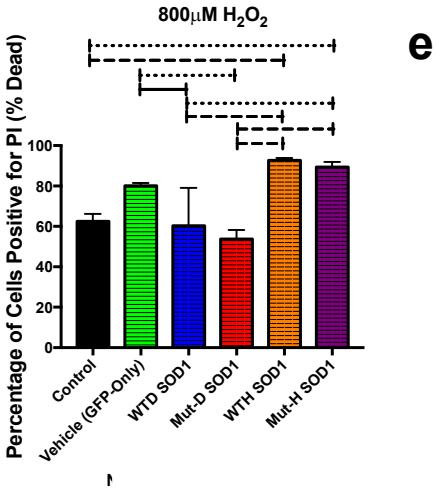
800μM H2O2
e
Percentage of Cells Positive for PI (% Dead)
100
80
60
40
20
0
Control
Vehicle (GFP-Only)
WTD SOD1
Mut-D SOD1
WTH SOD1
Mut-H SOD1

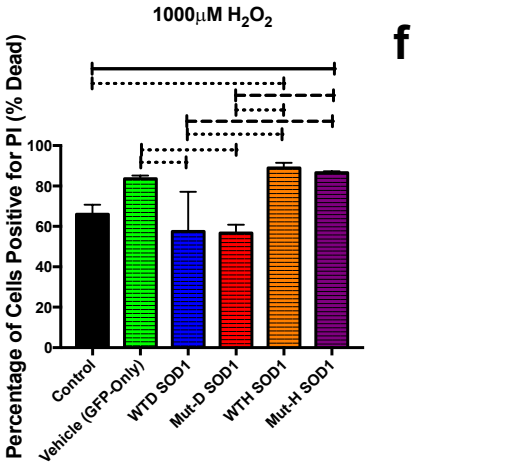
1000μM H2O2
f
Percentage of Cells Positive for PI (% Dead)
100
80
60
40
20
0
Control
Vehicle (GFP-Only)
WTD SOD1
Mut-D SOD1
WTH SOD1
Mut-H SOD1

Figure 6 A-C: Mitochondrial morphology descriptors (Aspect Ratio and Form Factor) of virally-transduced HEK-293T cells expressing different veterinary SOD1 variants (wild-type dog (E40) SOD1 (WTD), mutant dog (K40) SOD1 (Mut-D), wild-type horse (K40) SOD1 (WTH) and mutant horse (E40) SOD1 (Mut-H)) with appropriate vehicle and non-virally transduced control cells. The mean ± standard deviation of each morphological descriptor, per condition, is represented by the horizontal bar and error bars, respectively. The morphology values for each cell (minimum of 10 cells, 4 wells per condition) are displayed. The solid black bars represent a $p<0.05$; from a mixed model with post-hoc correction including the well number as a co-variant. Cells expressing the mutant dog SOD1 showed a significantly increased form factor (mean±SD: 1.439+0.1565), suggesting that the mitochondrial network was longer and more highly branched, compared to the cells expressing the wild-type dog SOD1 (1.356±0.09086) ($p=0.00507$). D: This can be appreciated in the representative confocal images of cells expressing wild-type dog SOD1 (WTD SOD1) or mutant dog SOD1 showing greater branching of the mitochondrial network (MitoTracker® Red) in the mutant dog SOD1 expressing cells. Transduced cells are revealed by positive GFP expression (green) and nuclei are stained by DAPI and coloured blue. White scale bar = 10μm.

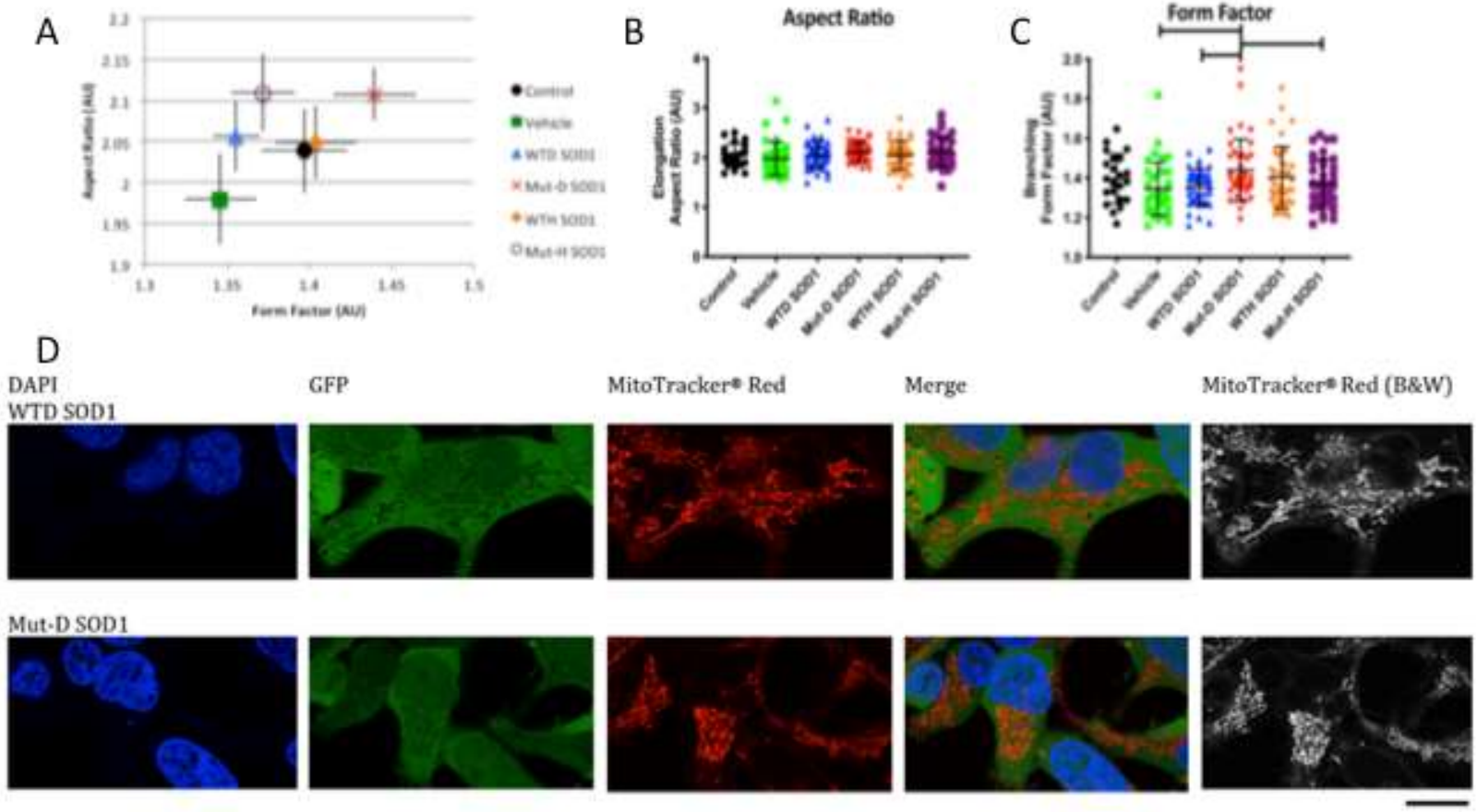
A
Form Factor (AU)
Control
Vehicle
WTD SOD1
Mut-D SOD1
WTH SOD1
Mut-H SOD1
B
Aspect Ratio
C
Form Factor
D
DAPI
GFP
MitoTracker® Red
Merge
MitoTracker® Red (B&W)
WTD SOD1
Mut-D SOD1

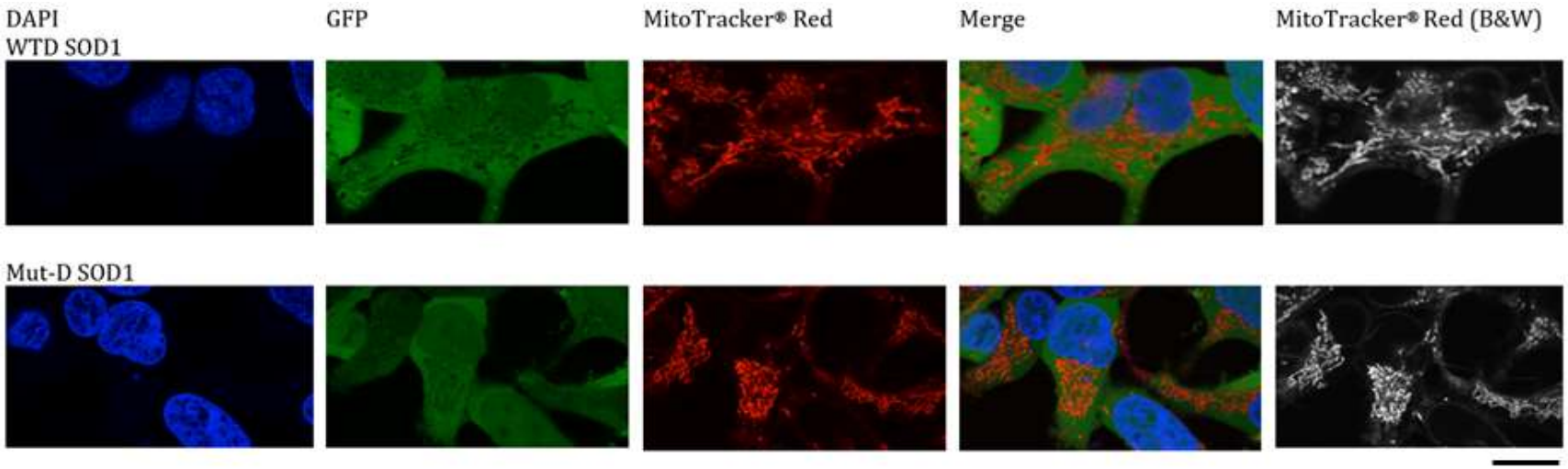
DAPI
GFP
MitoTracker® Red
Merge
MitoTracker® Red (B&W)
WTD SOD1
Mut-D SOD1

Figure 7 Summary of mitochondrial membrane potential (ΔΨm) (A: Confocal microscopy and B: Flow cytometry), ATP levels (C) and mitochondrial-derived superoxide ion levels (D) from virally-transduced cells expressing different SOD1 variants (wild-type dog (E40) SOD1 (WTD), mutant dog (K40) SOD1 (Mut-D), wild-type horse (K40) SOD1 (WTH) and mutant horse (E40) SOD1 (Mut-H)) with appropriate vehicle and non-virally transduced control cells. Solid black line represents statistical differences of $P < .05$ and the dotted black line represents statistical differences of $P < .001$

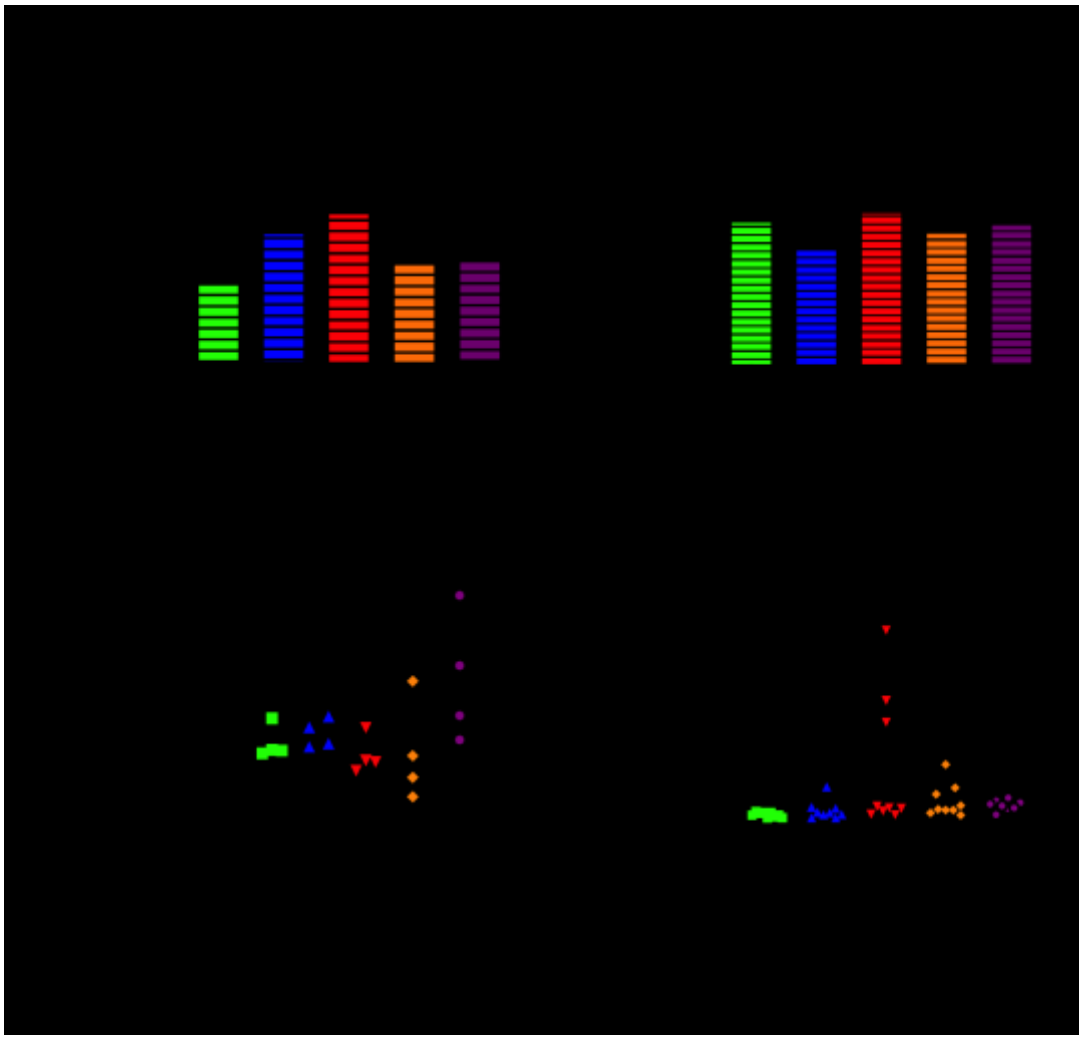

Supplementary Table 1: The volume of the mitochondrial networks in cells expressing different SOD1 variants, with vehicle and non-transduced controls were not significantly different from each other ($p>0.05$). The SOD1 variants included the wild-type dog SOD1 (E40) (WTD), mutant dog SOD1 (K40) (Mut-D), wild-type horse SOD1 (K40) (WTH) and mutant horse SOD1 (E40) (Mut-H).

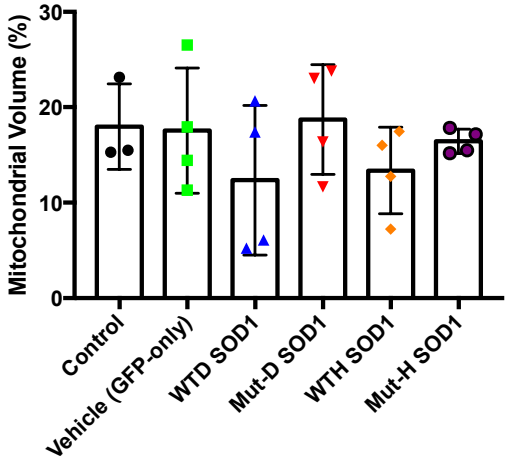

References:

1. Bento-Abreu, A., et al., *The neurobiology of amyotrophic lateral sclerosis.* Eur J Neurosci, 2010. **31**(12): p. 2247-65.

2. Rosen, D.R., *Mutations in Cu/Zn superoxide dismutase gene are associated with familial amyotrophic lateral sclerosis.* Nature, 1993. **364**(6435): p. 362.

3. Awano, T., et al., *Genome-wide association analysis reveals a SOD1 mutation in canine degenerative myelopathy that resembles amyotrophic lateral sclerosis.* Proc Natl Acad Sci U S A, 2009. **106**(8): p. 2794-9.

4. Katz, M.L., et al., *Cervical spinal cord and motor unit pathology in a canine model of SOD1-associated amyotrophic lateral sclerosis.* J Neurol Sci, 2017. **378**: p. 193-203.

5. Boillée, S., C. Vande Velde, and D.W. Cleveland, *ALS: a disease of motor neurons and their nonneuronal neighbors.* Neuron, 2006. **52**(1): p. 39-59.

6. Miosge, L.A., et al., *Comparison of predicted and actual consequences of missense mutations.* Proc Natl Acad Sci U S A, 2015. **112**(37): p. E5189-98.

7. Ivansson, E.L., et al., *Variants within the SP110 nuclear body protein modify risk of canine degenerative myelopathy.* Proc Natl Acad Sci U S A, 2016. **113**(22): p. E3091-100.

8. Windley, Z., *Comparative Functional and Morphological Effects of SOD-1 Mutations*, in *Comparative Biomedical Sciences*. 2012, Royal Veterinary College, University of London: London. p. 94.

9. Orlando, L., et al., *Recalibrating Equus evolution using the genome sequence of an early Middle Pleistocene horse.* Nature, 2013. **499**(7456): p. 74-8.

10. Mohammed, H.O., et al., *Epidemiology of equine motor neuron disease.* Vet Res, 1994. **25**(2-3): p. 275-8.

11. Draper, A.C.E. and R.J. Piercy, *Pathological classification of equine recurrent laryngeal neuropathy.* J Vet Intern Med, 2018. **32**(4): p. 1397-1409.

12. Librado, P., et al., *Ancient genomic changes associated with domestication of the horse.* Science, 2017. **356**(6336): p. 442-445.

13. Finno, C.J. and S.J. Valberg, *A comparative review of vitamin E and associated equine disorders.* J Vet Intern Med, 2012. **26**(6): p. 1251-66.

14. Maile, C.A., et al., *A highly prevalent equine glycogen storage disease is explained by constitutive activation of a mutant glycogen synthase.* Biochim Biophys Acta Gen Subj, 2017. **1861**(1 Pt A): p. 3388-3398.

15. McCue, M.E., et al., *Glycogen synthase (GYS1) mutation causes a novel skeletal muscle glycogenosis.* Genomics, 2008. **91**(5): p. 458-66.

16. Naylor, R.J., et al., *Allele copy number and underlying pathology are associated with subclinical severity in equine type 1 polysaccharide storage myopathy (PSSM1).* PLoS One, 2012. **7**(7): p. e42317.

17. Parge, H.E., R.A. Hallewell, and J.A. Tainer, *Atomic structures of wild-type and thermostable mutant recombinant human Cu,Zn superoxide dismutase.* Proc Natl Acad Sci U S A, 1992. **89**(13): p. 6109-13.

18. Miao, L. and D.K. St Clair, *Regulation of superoxide dismutase genes: implications in disease.* Free Radic Biol Med, 2009. **47**(4): p. 344-56.

19. Crisp, M.J., et al., *Canine degenerative myelopathy: biochemical characterization of superoxide dismutase 1 in the first naturally occurring non-human amyotrophic lateral sclerosis model.* Exp Neurol, 2013. **248**: p. 1-9.

20. Saccon, R.A., et al., *Is SOD1 loss of function involved in amyotrophic lateral sclerosis?* Brain, 2013. **136**(Pt 8): p. 2342-58.

21. Crown, A.M., Roberts, B.L., Crosby, K. et al. *Experimental Mutations in Superoxide Dismutase 1 Provide Insight into Potential Mechanisms Involved in Aberrant Aggregation in Familial Amyotrophic Lateral Sclerosis*. G3 (Bethesda), 2019. **9**(3): 719- 728.

22. Green, S.L., et al., *Structure, chromosomal location, and analysis of the canine Cu/Zn superoxide dismutase (SOD1) gene.* J Hered, 2002. **93**(2): p. 119-24.

23. Zimmerman, M.C., L.W. Oberley, and S.W. Flanagan, *Mutant SOD1-induced neuronal toxicity is mediated by increased mitochondrial superoxide levels.* J Neurochem, 2007. **102**(3): p. 609-18.

24. Richardson, K., et al., *The effect of SOD1 mutation on cellular bioenergetic profile and viability in response to oxidative stress and influence of mutation-type.* PLoS One, 2013. **8**(6): p. e68256.

25. Wang, H., et al., *ALS-associated mutation SOD1(G93A) leads to abnormal mitochondrial dynamics in osteocytes.* Bone, 2018. **106**: p. 126-138.

26. Khetan, S., et al., *Degradation-mediated cellular traction directs stem cell fate in covalently crosslinked three-dimensional hydrogels.* Nat Mater, 2013. **12**(5): p. 458-65.

27. Hoerndli, F.J., et al., *Reference genes identified in SH-SY5Y cells using custom-made gene arrays with validation by quantitative polymerase chain reaction.* Anal Biochem, 2004. **335**(1): p. 30-41.

28. Hildyard, J.C. and D.J. Wells, *Identification and validation of quantitative PCR reference genes suitable for normalizing expression in normal and dystrophic cell culture models of myogenesis.* PLoS Curr, 2014. **6**.

29. Hildyard, J.C.W., et al., *Determination of qPCR Reference Genes Suitable for Normalizing Gene Expression in a Canine Model of Duchenne Muscular Dystrophy.* J Neuromuscul Dis, 2018. **5**(2): p. 177-191.

30. Schindelin, J., et al., *Fiji: an open-source platform for biological-image analysis.* Nat Methods, 2012. **9**(7): p. 676-82.

31. Innovagen. *Innovagen Protein Calculator*. 2015 [cited 2018; Available from: https://pepcalc.com/protein-calculator.php.

32. Kobatake, Y., et al., *Localization of a mutant SOD1 protein in E40K-heterozygous dogs: Implications for non-cell-autonomous pathogenesis of degenerative myelopathy.* J Neurol Sci, 2017. **372**: p. 369-378.

33. Perry, S.W., et al., *Mitochondrial membrane potential probes and the proton gradient: a practical usage guide.* Biotechniques, 2011. **50**(2): p. 98-115.

34. Hayyan, M., M.A. Hashim, and I.M. AlNashef, *Superoxide Ion: Generation and Chemical Implications.* Chem Rev, 2016. **116**(5): p. 3029-85.

35. Nakamae, S., et al., *Accumulation and aggregate formation of mutant superoxide dismutase 1 in canine degenerative myelopathy.* Neuroscience, 2015. **303**: p. 229-40.

36. Stevens, J.C., et al., *Modification of superoxide dismutase 1 (SOD1) properties by a GFP tag--implications for research into amyotrophic lateral sclerosis (ALS).* PLoS One, 2010. **5**(3): p. e9541.

37. Keskin, I., et al., *Comprehensive analysis to explain reduced or increased SOD1 enzymatic activity in ALS patients and their relatives.* Amyotroph Lateral Scler Frontotemporal Degener, 2017. **18**(5-6): p. 457-463.

38. Henriques, S.F., et al., *Different outcome of sarcoglycan missense mutation between human and mouse.* PLoS One, 2018. **13**(1): p. e0191274.

39. Kobuke, K., et al., *A common disease-associated missense mutation in alpha-sarcoglycan fails to cause muscular dystrophy in mice.* Hum Mol Genet, 2008. **17**(9): p. 1201-13.

40. Polymeropoulos, M.H., et al., *Mutation in the alpha-synuclein gene identified in families with Parkinson's disease.* Science, 1997. **276**(5321): p. 2045-7.

41. Kaufmann, W., et al., *Proliferative and nonproliferative lesions of the rat and mouse central and peripheral nervous systems.* Toxicol Pathol, 2012. **40**(4 Suppl): p. 87S-157S.

42. Munch, C. and A. Bertolotti, *Exposure of hydrophobic surfaces initiates aggregation of diverse ALS-causing superoxide dismutase-1 mutants.* J Mol Biol, 2010. **399**(3): p. 512-25.

43. Munch, C., J. O'Brien, and A. Bertolotti, *Prion-like propagation of mutant superoxide dismutase-1 misfolding in neuronal cells.* Proc Natl Acad Sci U S A, 2011. **108**(9): p. 3548-53.

44. Prudencio, M., et al., *Variation in aggregation propensities among ALS-associated variants of SOD1: correlation to human disease.* Hum Mol Genet, 2009. **18**(17): p. 3217-26.

45. Keskin, I., et al., *Effects of Cellular Pathway Disturbances on Misfolded Superoxide Dismutase-1 in Fibroblasts Derived from ALS Patients.* PLoS One, 2016. **11**(2): p. e0150133.

46. Grad, L.I., et al., *Intercellular propagated misfolding of wild-type Cu/Zn superoxide dismutase occurs via exosome-dependent and -independent mechanisms.* Proc Natl Acad Sci U S A, 2014. **111**(9): p. 3620-5.

47. Chiti, F., et al., *Rationalization of the effects of mutations on peptide and protein aggregation rates.* Nature, 2003. **424**(6950): p. 805-8.

48. Tiwari, A., Z. Xu, and L.J. Hayward, *Aberrantly increased hydrophobicity shared by mutants of Cu,Zn-superoxide dismutase in familial amyotrophic lateral sclerosis.* J Biol Chem, 2005. **280**(33): p. 29771-9.

49. Abdolvahabi, A., et al., *Arresting amyloid with coulomb's law: acetylation of ALS-linked SOD1 by aspirin impedes aggregation.* Biophys J, 2015. **108**(5): p. 1199-212.

50. Shi, Y., A. Abdolvahabi, and B.F. Shaw, *Protein charge ladders reveal that the net charge of ALS-linked superoxide dismutase can be different in sign and magnitude from predicted values.* Protein Sci, 2014. **23**(10): p. 1417-33.

51. Goldsteins, G., et al., *Deleterious role of superoxide dismutase in the mitochondrial intermembrane space.* J Biol Chem, 2008. **283**(13): p. 8446-52.

52. Mortiboys, H., et al., *Mitochondrial function and morphology are impaired in parkin-mutant fibroblasts.* Ann Neurol, 2008. **64**(5): p. 555-65.

53. Koopman, W.J., et al., *Inhibition of complex I of the electron transport chain causes O2-. -mediated mitochondrial outgrowth.* Am J Physiol Cell Physiol, 2005. **288**(6): p. C1440-50.

54. Deheshi, S., et al., *Changes in mitochondrial morphology induced by calcium or rotenone in primary astrocytes occur predominantly through ros-mediated remodeling.* J Neurochem, 2015. **133**(5): p. 684-99.

55. Koopman, W.J., et al., *Mammalian mitochondrial complex I: biogenesis, regulation, and reactive oxygen species generation.* Antioxid Redox Signal, 2010. **12**(12): p. 1431-70.

56. Coussee, E., et al., *G37R SOD1 mutant alters mitochondrial complex I activity, Ca(2+) uptake and ATP production.* Cell Calcium, 2011. **49**(4): p. 217-25.

57. Li, Q., et al., *ALS-linked mutant superoxide dismutase 1 (SOD1) alters mitochondrial protein composition and decreases protein import.* Proc Natl Acad Sci U S A, 2010. **107**(49): p. 21146-51.

58. Li, N., et al., *Mitochondrial complex I inhibitor rotenone induces apoptosis through enhancing mitochondrial reactive oxygen species production.* J Biol Chem, 2003. **278**(10): p. 8516-25.

59. Dlaskova, A., et al., *Mitochondrial Complex I superoxide production is attenuated by uncoupling.* Int J Biochem Cell Biol, 2008. **40**(10): p. 2098-109.

60. Detmer, S.A. and D.C. Chan, *Functions and dysfunctions of mitochondrial dynamics.* Nat Rev Mol Cell Biol, 2007. **8**(11): p. 870-9.

61. Coates, J.R. and F.A. Wininger, *Canine degenerative myelopathy.* Vet Clin North Am Small Anim Pract, 2010. **40**(5): p. 929-50.

62. Abu-Hamad, S., et al., *Misfolded SOD1 Accumulation and Mitochondrial Association Contribute to the Selective Vulnerability of Motor Neurons in Familial ALS: Correlation to Human Disease.* ACS Chem Neurosci, 2017. **8**(10): p. 2225-2234.

63. Raimondi, A., et al., *Cell culture models to investigate the selective vulnerability of motoneuronal mitochondria to familial ALS-linked G93ASOD1.* Eur J Neurosci, 2006. **24**(2): p. 387-99.

64. Votion, D.-M., et al. *Physical fitness and mitochondrial respiratory capacity in horse skeletal muscle*. PLoS ONE, 2012; **7**(4): e34890.

65. Lee, D.Y., et al., *Modulation of SOD1 Subcellular Localization by Transfection with Wild- or Mutant-type SOD1 in Primary Neuron and Astrocyte Cultures from ALS Mice.* Exp Neurobiol, 2015. **24**(3): p. 226-34.

66. Milani, P., et al., *SOD1 Transcriptional and Posttranscriptional Regulation and Its Potential Implications in ALS.* Neurol Res Int, 2011. **2011**: p. 458427.

67. Ge, W.W., et al., *Neuronal tissue-specific ribonucleoprotein complex formation on SOD1 mRNA: alterations by ALS SOD1 mutations.* Neurobiol Dis, 2006. **23**(2): p. 342-50.

68. Berglund, A.C., et al. *RBPDB: The database of RNA-binding specificities*. 2018; Available from: http://rbpdb.ccbr.utoronto.ca/index.php.

69. Chung, C.Y., et al., *Aberrant activation of non-coding RNA targets of transcriptional elongation complexes contributes to TDP-43 toxicity.* Nat Commun, 2018. **9**(1): p. 4406.

70. Goodwin, M., et al., *MBNL Sequestration by Toxic RNAs and RNA Misprocessing in the Myotonic Dystrophy Brain.* Cell Rep, 2015. **12**(7): p. 1159-68.

Supplementary Data

Table 1: Primer Sequences

SOD1 Genotyping in Different Perissodactyla Species and Horse Breeds
Primer sequences used for SOD1 Exon 2 amplification (5'-3'):

Equine SOD-1 Exon 2 Forward 1	CACTTGCTCTCTCAAACTTGT	Przewalski's horse, Horse Breeds
Equine SOD-1 Exon 2 Reverse 1	TAGCAGTCATACTGACTTGACC	Przewalski's horse, Horse Breeds
Equine SOD-1 Exon 2 Forward 3	GTCGTTCTGAAGGGATTCAT	Onager, Chapman's Zebra, Donkey, Malaysian Tapir
Equine SOD-1 Exon 2 Reverse 3	CTTGTGTATTATCTCCAAACTCGT	Onager, Chapman's Zebra, Donkey, Malaysian Tapir

Mutagenesis:
Primer sequences used for mutagenesis (5'-3'):

Horse SOD1 K40 Forward	CTGTGGTCCCTTCGGATCTC
Horse SOD1 K40 Reverse	CTAGGACTCAGACCATGACAC

qPCR Primers
Primer sequences used for qPCR (all 5' to 3'):

Human GAPDH Forward	ATTCCACCCATGGCAAATTC
Human GAPDH Reverse	GGGATTTCCATTGATGACAAGC
Human POLR2F Forward	CCCGAAAGATCCCCATCAT
Human POLR2F Reverse	CACCCCCCAGTCTTCATAGC
Human MPRIP Forward	ATCTCAGCCATCGAAGCCAT
Human MPRIP Reverse	TGGCTCTTCTCCAGCTCCC
Dog SOD1 Forward	AAGTGGGCCTGTTGTGGTAT
Dog SOD1 Reverse	ATCCTTGCCAGCAGTCACAT
Horse SOD1 Forward	ACCAAAGGCGATCACGGATT
Horse SOD1 Reverse	ATCAGCAGTCACATTGCCCA
Human SOD1 Forward	ATGGACCAGTGAAGGTGTGG
Human SOD1 Reverse	CTTTGGCCCACCGTGTTTTC

Figure 1: Exon 2 fragment of SOD1 sequencing in 7 different horse breeds, centred around the 40th codon (red lines), showing the conservation of the lysine (K) residue at this locus.

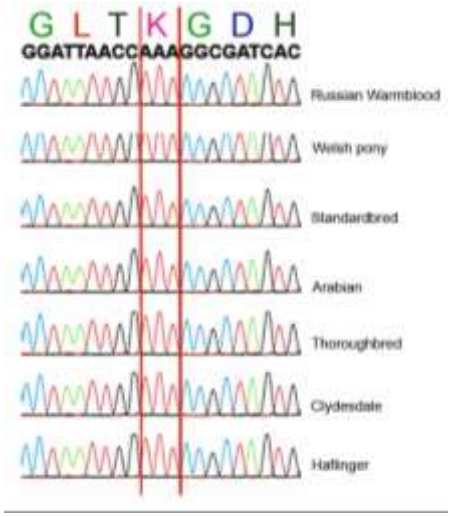

Figure 2: The volume of the mitochondrial networks in cells expressing different SOD1 variants, with vehicle and non-transduced controls were not significantly different from each other ($p>0.05$). The SOD1 variants included the wild-type dog SOD1 (E40) (WTD), mutant dog SOD1 (K40) (Mut-D), wild-type horse SOD1 (K40) (WTH) and mutant horse SOD1 (E40) (Mut-H).

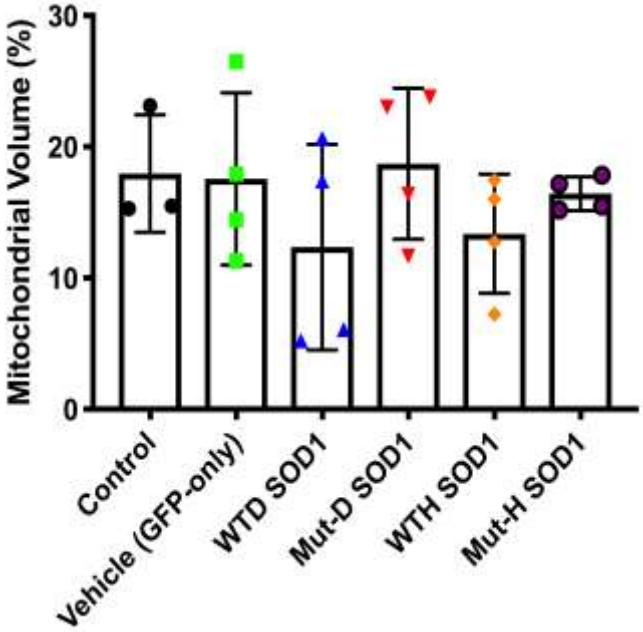

Figure 3: Relative expression of dog SOD1 (WTD (E40) and Mut-D (K40)) and horse SOD1 (WTH (K40) and Mut-H (E40)) mRNA in virally transduced SHSY5Y cells, normalised to GADPH, MPRIP and POLR2F expression identified with specific primers to horse SOD1. The relative expression of WTH SOD1 and Mut-H SOD1 were comparable to one another ($p>0.05$) mirroring the protein expression results. Negligible expression of horse SOD1 was seen in control, vehicle, WTD- and Mut-D-expressing cells. Data is expressed as the mean $\pm$ standard deviation from experimental replicates (n=3). Different letters indicate statistically significant differences between groups ($p<0.05$) and were generated from One-way ANOVA statistical analysis with post-hoc testing.